Optical Materials 39 (2015) 118–124

Contents lists available at ScienceDirect

Optical Materials

journal homepage: www.elsevier.com/locate/optmat

Synthesis and fabrication of silver nanowires embedded in PVP fibers by near-field electrospinning process

T.L. Yang [a,b], C.T. Pan [a,b,*], Y.C. Chen [a,b], L.W. Lin [c], I.C. Wu [a,b], K.H. Hung [a,b], Y.R. Lin [a,b], H.L. Huang [d], C.F. Liu [d], S.W. Mao [d], S.W. Kuo [e]

[a] Department of Mechanical and Electro-Mechanical Engineering, Center for Nanoscience & Nanotechnology, National Sun Yat-Sen University, Kaohsiung 80424, Taiwan
[b] National Science Council Core Facilities Laboratory for Nano-Science and Nano-Technology in Kaohsiung-Pingtung Area, Taiwan
[c] Mechanical Engineering Department and Department of Mechanical Engineering and Berkeley Sensor and Actuator Center, University of California, Berkeley, CA 94720, USA
[d] Department of Mechanical Engineering, Republic of China Military Academy, Kaohsiung 83059, Taiwan
[e] Department of Materials and Optoelectronics Science, National Sun Yat-Sen University, Kaohsiung 80424, Taiwan

A R T I C L E I N F O

Article history:
Received 10 August 2014
Received in revised form 4 November 2014
Accepted 7 November 2014
Available online 26 November 2014

Keywords:
Near-field
Electrospinning
PVP
AgNWs
Transparent conductive

A B S T R A C T

In this study, polyol process was used to synthesize anisotropic silver nanowires (AgNWs). The ranges of synthesis temperature from 100 to 200 degrees were explored, and the ranges from 4.53 to 13.75 wt% Polyvinylpyrrolidone (PVP) were investigated. The lengths and diameters of AgNWs from 15 to 30 μm and from 10 to 50 nm can be obtained, respectively. Then, the AgNWs embedded in PVP fibers (PVP/AgNWs) were fabricated by the near-field electrospinning (NFES) process. The AgNWs were broken down into nanoparticles when the applied electric field was over 1.4×10^7 V/m. However, the AgNWs could remain undamaged when the electric field was controlled between 8×10^6 and 1.2×10^7 V/m. Therefore, the threshold electric field can be determined and the diameter of the PVP/AgNWs fibers from 500 nm to 10 μm can be obtained. Next, the characteristics of the PVP/AgNWs were examined by N&K analyzer, four-point probe, EDS and FTIR. The transmittance of PVP/AgNWs films was 51.29–68.97% and the sheet resistance of purified AgNWs was 0.125 Ω/sq which was superior to that of commercial ITO. In addition, the haze of PVP/AgNWs with 30–90 nm thick was from 11.5% to 13.3%. In the near future, the PVP/AgNWs fibers can be used as transparent conductive electrodes.

1. Introduction

Recently, as the smart display technology has been developing rapidly, lots of attention are focused on the application of the transparent electrodes [1,2], which can be widely applied to the smart phones [3,4], touch screen [2,5], organic light-emitting diode (OLED) [4], liquid crystal display (LCD) [6], and thin-film silicon solar cells. Currently, the important material of the current transparent electrodes was indium tin oxide (ITO) [7], but the indium was scarce on earth. Moreover, the disadvantages of ITO including expensive price, brittle material, and complicated process needed in the vacuum environment [8] resulted in extremely energy-intensive and economically expensive fabrication process. Therefore, the new materials for transparent conductive electrodes should be developed to replace the ITO [9].

There are many drawbacks of the ITO transparent electrodes. Therefore, some emerging alternatives, such as carbon nanotubes [10], graphene [11] and silver nanowires (AgNWs) [12] with high conductivity and transmittance were studied to replace the ITO. AgNWs are a promising alternative, which have been reported as the potential candidate to replace ITO. This material was pioneered by Lee et al [13] and showed that the transparent electrodes fabricated by casting AgNWs thin film exhibited comparable and even better than that fabricated by sputter-coated ITO. Now, several methods for the syntheses of AgNWs have been developed such as chemical synthesis, electrochemical process, hydrothermal method, ultraviolet irradiation photodetection technique, DNA template, porous materials template, and polyol process [14,15]. In addition, far-field electrostatic spraying system was used to obtain AgNWs electrodes [14]. However, a high voltage at the tip was required.

The electrospinning is a technology where a high electric field is used to produce nonwoven materials which are excellent in the characteristics such as controllable porosity, high surface area, and uniformity of the fibers [16]. In this process, a high voltage

* Corresponding author at: Department of Mechanical and Electro-Mechanical Engineering, National Sun Yat-Sen University, No. 70 Lien-hai Rd., Kaohsiung 80424, Taiwan. Tel.: +886 7 5252000x4239; fax: +886 7 5254299.
E-mail address: ligalab@gmail.com (C.T. Pan).

http://dx.doi.org/10.1016/j.optmat.2014.11.009
0925-3467/

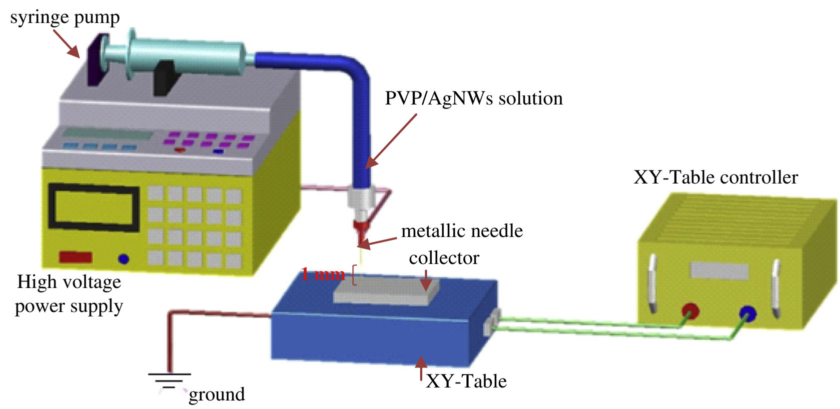

Fig. 1. The experimental set-up of near-field electrospinning system.

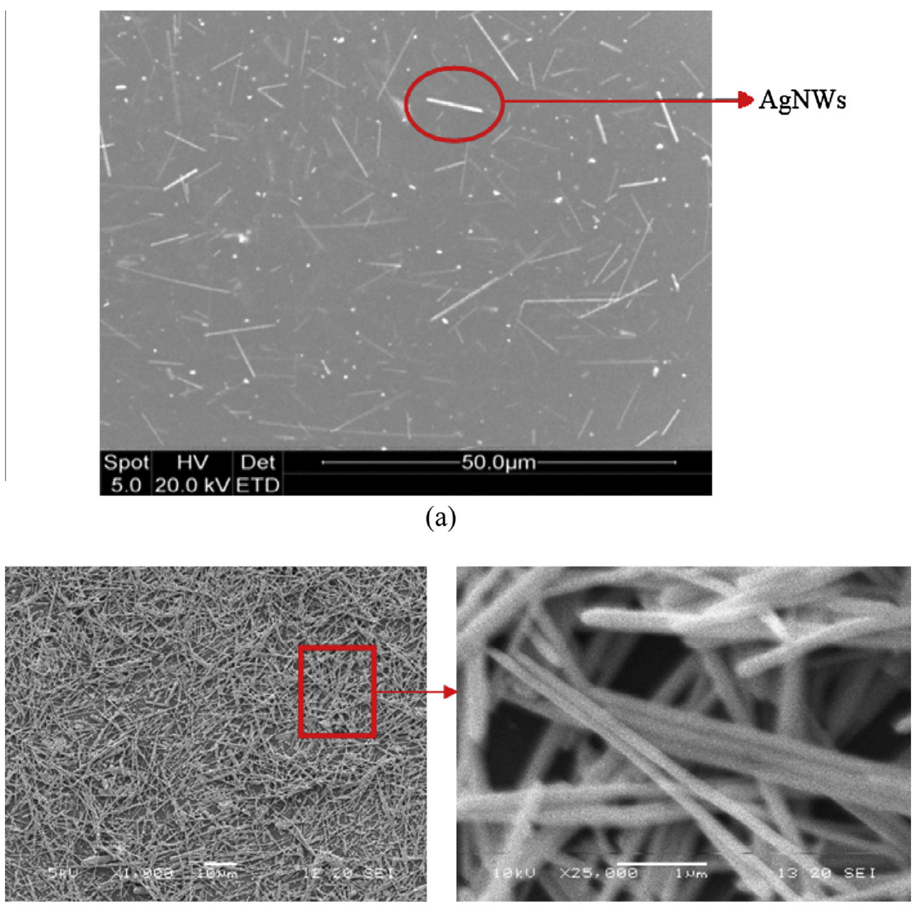

Fig. 2. The images of, (a) PVP/AgNWs and, (b) centrifuged AgNWs.

was applied to a metallic capillary which was connected to a reservoir holding a polymer solution with the proper viscosity, conductivity and surface tension [17]. A positive potential was applied to a metal wire which was connected with the glass pipette filled with polymer solution. Thus, the polymer solution can be electrospun (electric field strength was 100 kV/m) [18]. In another study, the fibers could be direct-written Polyethylene oxide (PEO) fibers in a special pattern by using near-field electrospinning (NFES) with a programmable collector [19,20]. To achieve continuous NFES process, a critical voltage was applied to deform a polymer meniscus by electrospinning process [21]. In the energy scavenging applications, the NFES was used to polarize PVDF fibers in situ and transform non-polar α phase into polar β phase [22]. When a DC voltage bias was set at 14 kV and the tube rotation velocity was set at 1900 rpm, piezoelectric PVDF fibers with small diameters and smooth surface morphology can be obtained [23]. The PVDF fibers showed a downward center displacement of 23 μm and upward center displacement of 16 μm under a high electric field [24]. D. Di Camillo et al adopted NFES process at 1.1 kV and PEO-TiO_2 polymer solution to make NO_2 nanofibers sensor which can detect limits as low as 1 ppm [25]. Min et al fabricated organic FET nanofibers with a low contact resistance (<5.53 Ω/cm) by using

(a) (b) (c)

Fig. 3. The images of, (a) the AgNWs before NFES process and (a) the AgNWs after NFES at 20 kV and (a) at 14 kV.

NFES process at 3–4 kV [26]. In 2013, Di Camillo et al successfully applied NFES process at 1.3 kV to make MEH-PPV/PEO conjugated polymer light-emitting nanofibers [27]. Mayousse et al developed AgNWs electrodes by adopting NaCl seed to prepare AgNWs with 2–25 μm long and 40–80 nm in diameter for a quadrupole sensing circuit [28].

In this study, the polyol reduction method was adopted. The $AgNO_3$ was added as the source of Ag ion, and then the ethylene glycol (EG) was added as reducing agent at 170 °C. The Polyvinylpyrrolidone (PVP) was used as surfactant which can limit the growth direction of AgNWs to one dimension [29]. During the NFES, the electric field applied to electrospin the PVP/AgNWs fibers was set as 8×10^6–1.2×10^7 V/m which was lower than that of the far-field electrostatic spraying system. Lower electric field resulted in fewer AgNWs broken. Then, the composite fibers of PVP/AgNWs were orderly collected. The characteristics of nanocomposite fibers were analyzed and measured by the instruments such as Scanning Electron Microscope (SEM, FEI QUANTA 200TSM-5510) to observe the morphology, Energy dispersive X-ray (EDS) and Fourier transform infrared spectroscopy (FTIR) to analyze the ingredient of PVP/AgNWs. In addition, the optical transmittance and sheet resistance were measured by N&K analyzer and four-point probe. The optical haze was measured by ASTM D1003 standard. The luminance of LEDs with various conductive electrodes such as copper, AgNWs and silver colloid were measured and analyzed.

2. Experimental details

2.1. Synthesis of PVP/AgNWs solution

The AgNWs were synthesized using polyol process with some modifications. At first, the mixture of 0.276 g PVP (M_w is 1,300,000, powder) and 5 ml ethylene glycol (EG) was heated up to 170 °C and stirred by magnet at 450–600 rpm simultaneously. After the PVP was dissolved completely in the EG, 0.05 g AgCl (99.999%) was added in the solution. Then, $AgNO_3$ (99.0%) was added in the solution. The solution was kept stirring and heating to make the AgNWs grow completely, and then the PVP/AgNWs solution was cooled down to the room temperature.

2.2. Electrospinning of PVP/AgNWs composite fibers

The syringe with a 0.5 mm diameter metallic needle was filled with PVP/AgNWs solution. Then, the electrode of a high voltage power supply (YOU-SHANG Technical Corp) was attached to the metallic needle tip and the applied voltage was set from 8 to 12 kV. Moreover, the syringe was horizontally installed on the syringe pump (Model: KDS-100, KDScientific) which can control the flow rate at 10 μl h^{-1}. Next, the tip-to-collector distance was set at 1 mm. The silicon or glass collector grounded by copper tapes was put on the XY-Table controlled by a programmable system. Fig. 1 shows schematically the experimental set-up. The droplet was dragged out by the electrical field to form a Taylor cone where

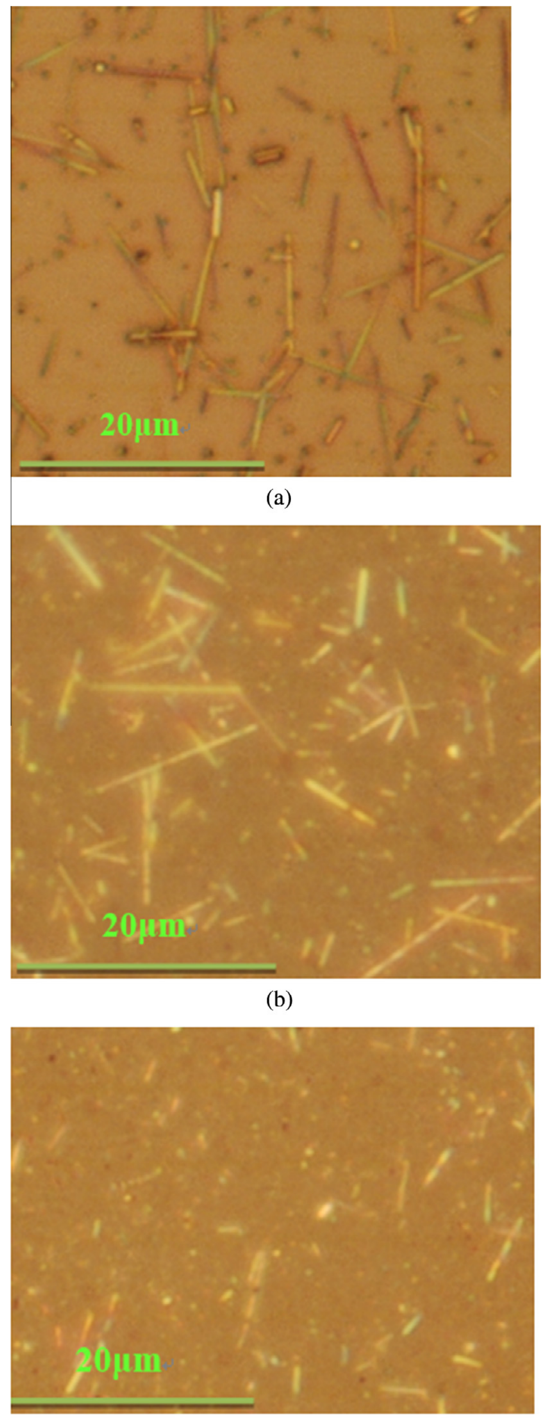

(a)
(b)
(c)

Fig. 4. The images of PVP/AgNWs fibers electrospun at, (a) suitable 8 kV, (b) 14 kV and, (c) 20 kV.

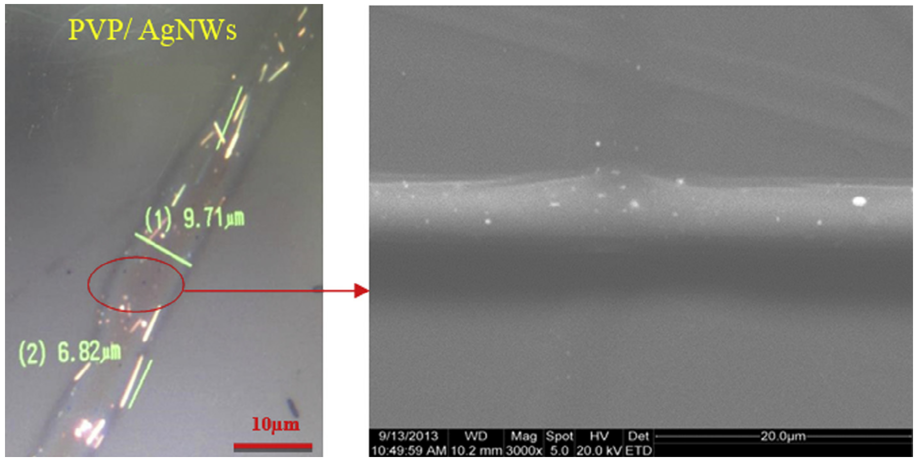

(a) OM (b) SEM

Fig. 5. The as-electrospun PVP/AgNWs fibers with 9–10 μm in diameters.

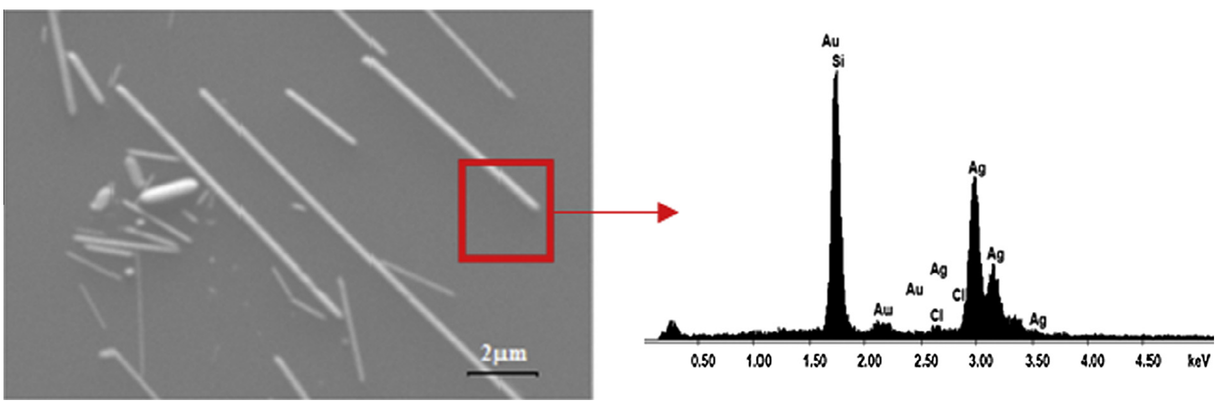

Fig. 6. EDS spectrum of PVP/AgNWs fibers.

the solution were electrospun out to form PVP/AgNWs composite fibers.

3. Results and discussion

3.1. Results of synthesis of PVP/AgNWs solution

Fig. 2(a) shows the uniformly formulated PVP/AgNWs solution where AgNWs can be seen clearly. Then, the as-prepared solution was centrifuged and dried at a high temperature in order to remove PVP. Fig. 2(b) shows the SEM of the centrifuged AgNWs. The diameters and lengths of AgNWs were ranging from 10 to 50 nm and 15 to 30 μm, respectively.

3.2. Broken AgNWs due to high voltage

The synthesized PVP/AgNWs solution was electrospun using NFES process. The voltages were set from 14 to 20 kV and the distance between metallic needle and collector was set as 1 mm. Fig. 3(a) shows the morphology of the original AgNWs synthesized by the polyol synthesis. The AgNWs remain complete without being broken before the NFES process. But after the NFES process, there were many broken AgNWs observed in Fig. 3(b) when the applied voltage was set at voltage higher than 20 kV. Due to the high voltage, the electric charges were accumulated on the AgNWs and made them break down. When a lower applied voltage of 14 kV was set, there were less broken AgNWs observed. However, some burned AgNWs can be found, as shown in the circled part in Fig. 3(c).

3.3. The influence of different voltages on the AgNWs

Compared with the AgNWs electrospun at 8 kV voltage (see Fig. 4(a)), Fig. 4(b) shows that lots of broken AgNWs were observed when the applied voltage was set at 14 kV. Moreover, the AgNWs could be broken down to silver nanoparticles (AgNPs) which can make the amount of AgNWs decrease when the applied voltage increased. The Fig. 4(c) shows lots of AgNPs in the fibers at 20 kV.

After several experiments of the NFES process carried out, the optimal applied voltage was determined as 8–12 kV with 1 mm distance between collector and metallic needle. Fig. 5 shows that the AgNWs fibers with high aspect ratio can be obtained (i.e., 30–50 nm in diameter and 9–10 μm long).

3.4. EDS and XRD results

Fig. 6 shows the results of EDS analysis of PVP/AgNWs fibers. The AgNWs embedded in the fibers can be observed clearly. In addition, the Au element can be detected due to the coating for SEM observation, and the Si element was detected because of the silicon substrate. Moreover, the chlorine element was detected because of the residual chlorine of silver chloride functioned as the seed layer of AgNWs.

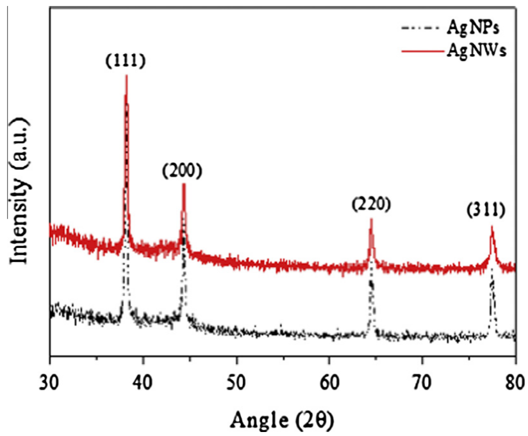

Fig. 7. Lattice plane measured by XRD.

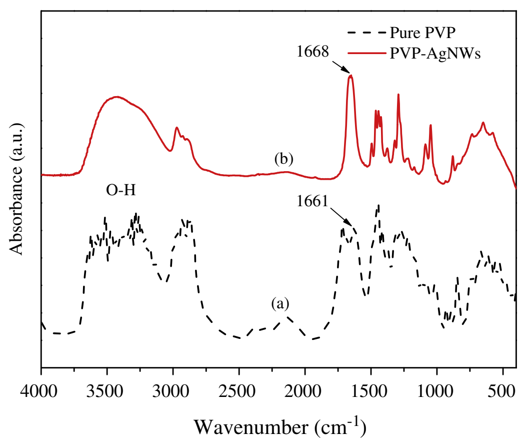

Fig. 8. Analysis of FTIR of the as-electrospun (a) pristine PVP fibers, (b) PVP/AgNWs fibers.

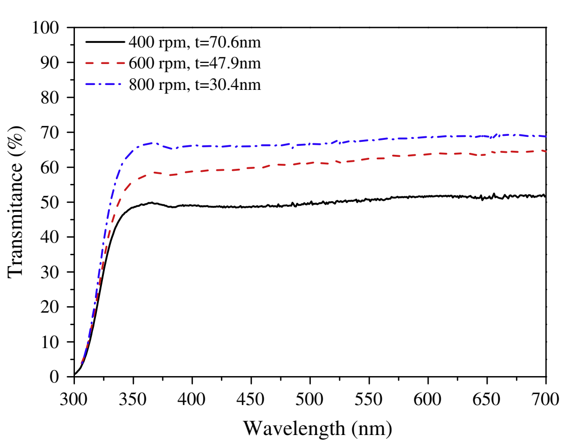

Fig. 9. Analysis of transmittance of PVP/AgNWs at 400, 600, and 800 rpm rotating speed.

Fig. 7 shows the XRD analysis of AgNWs and AgNPs. The red line represents the diffraction pattern of AgNWs and black dash line represents the diffraction pattern of AgNPs. From the diffraction patterns, the as-synthesized sample was confirmed to be Ag because the (111), (200), (220) and (311) lattice planes represented the diffraction peaks of Ag. The XRD pattern indicates that the high purity of face centered cube (FCC) silver can be prepared by polyol process.

Fig. 10. The measurement of the sheet resistance of silver nanowire film.

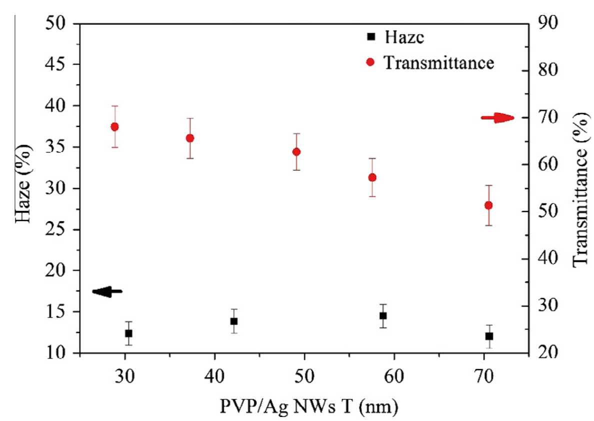

Fig. 11. The relationship between thickness, haze and transmittance of PVP/AgNWs films.

3.5. FTIR measurement

To understand the characteristic of the FTIR of PVP/AgNWs and make sure whether the ingredients of the as-electrospun PVP/AgNWs fibers changed or not, the PVP/AgNWs fibers were analyzed by FTIR. Fig. 8 shows the result of FTIR. The curve (A) and curve (B) were the spectra of the pristine PVP fibers and PVP/AgNWs fibers. The wavenumber of FTIR spectrum was ranging from 4000 cm^{-1} to 400 cm^{-1}. The 3450–3740 cm^{-1} was stretching vibration region of O—H because of moistures. The 1655–1670 cm^{-1} was stretching vibration region of C=O, 1020–1230 cm^{-1} was stretching vibration region of C—N, 1050–1250 cm^{-1} was stretching vibration region of C—O and 2700–3300 cm^{-1} was stretching vibration region of C—H [30].

The peak C=O at 1661 cm^{-1} in the curve (a) indicates the existence of PVP. In curve (b), the C=O peak was shifted from 1661 to 1668 cm^{-1}. It indicates that there was interaction between PVP and AgNWs where the AgNWs were encapsulated in the PVP. The purpose of PVP was to cover the AgNWs and make them grow anisotropically.

3.6. N&K analyzer measurement

The transmittance was one of the most crucial factors to PVP/AgNWs for the transparent conductive electrodes or circuits. To measure the transmittance, the transmittance of glass collector was taken into consideration. The transmittance of collector was

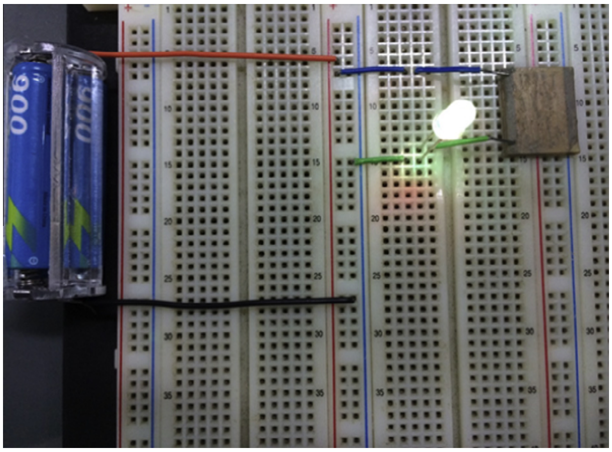

Fig. 12. The experimental configuration of LED circuits.

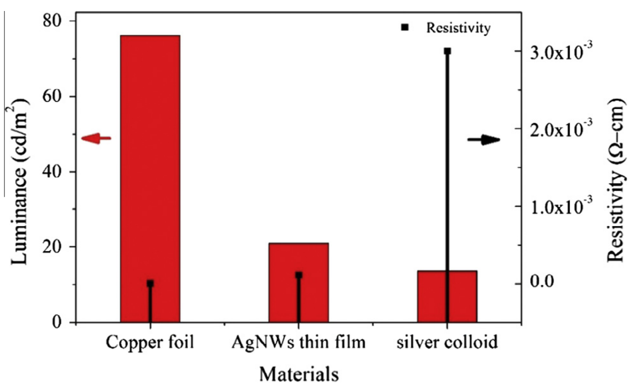

Fig. 13. The relationship between the resistivity and luminance.

set as the reference value of transmittance. Fig. 9 shows the wavelength of spectrometer scanned from 350 to 750 nm. The PVP/AgNWs solution was spin-coated on glass to form thin film at 400, 600 and 800 rpm spinning speed, respectively. The transmittance and thickness of PVP/AgNWs film at 400 rpm spinning speed were measured as 51.29% and 70.6 nm, respectively. The transmittance and thickness of PVP/AgNWs film at 600 rpm were measured as 63.91% and 47.9 nm, respectively. The transmittance and thickness of PVP/AgNWs film at 800 rpm were measured as 68.97% and 30.4 nm, respectively. The result shows that the best transmittance can be near 70%. The transmittance became higher because a higher spinning speed resulted in a smaller thickness of PVP/AgNWs films, which enhanced the transmittance.

3.7. Resistance measurement

The sheet resistance of PVP/AgNWs films deposited on the glass collector was measured by four-point probe. The sheet resistance was more than 1 MΩ/sq. However, when the PVP was removed by centrifugation to purify the AgNWs, Fig. 10 shows that the sheet resistance was measured down to 0.125 Ω/sq becasuse the PVP can isolate the AgNWs and increase the resistance [31].

3.8. Haze measurement

Based on ASTM D 1003 standard measurement, the haze values of different thicknesses of the PVP/AgNWs films were measured. Fig. 11 shows the relationship between the haze and transmittance of different thicknesses of PVP/AgNWs films. The haze was measured as 11.5–3.3% corresponding to the PVP/Ag/NWs thickness from 30 to 90 nm; and the corresponding transmittance was ranging from 51.29% to 68.97%. This result compared with the experimental results of Araki et al [32] shows the same trend.

3.9. Applications

The AgNWs have been attempted to apply on a LED electronic circuit. Fig. 12 shows the experimental configuration. We used different electrodes including the copper foil, silver colloid and the as-spun AgNWs film to measure the luminance of LED and resistivity of the electrodes. Fig. 13 shows the relationship between the resistance and luminance. The resistivity of copper foil, AgNWs film and commercial silver colloid were measured as 1.7×10^{-8} Ω cm, 1.11×10^{-4} Ω cm and 3×10^{-3} Ω cm, respectively. When copper foil was used as electrodes, the LED luminance value was measured as 7.619×10^1 cd/m^2; when silver colloid was used as electrodes, the LED luminance value was 1.364×10^1 cd/m^2; when AgNWs film was used as electrodes, the LED luminance value was 2.101×10^1 cd/m^2. This study found that when AgNWs film was used as electrodes, the luminance values was higher than that of commercial silver colloid. The AgNWs showed great potential to be applied as electrode material.

4. Conclusions

The PVA/AgNWs composite fibers have been successfully fabricated via the NFES process. A simple method was introduced to the preparation of organic–inorganic composite fibers. The centrifuged AgNWs show that the diameters and lengths of AgNWs were ranging from 10 to 50 nm and 15 to 30 μm, respectively. For the NFES process, when the applied voltage was more than 14 kV, AgNWs can be broken down. In addition, the amount of AgNPs increased in the fibers when a higher voltage was applied. By using the FTIR, the shifting of C=O peak indicated that the PVP attached on the surface of the AgNWs. The result of N&K analyzer shows that the transmittance of PVP/AgNWs film coated on the glass collector at 800 rpm spinning speed was better than that at 200 rpm. The sheet resistance of purified AgNWs was measured as 0.125 Ω/sq by four-point probe. The haze from 11.5% to 13.3% was measured with respect to the AgNWs thicknesses from 30 to 90 nm; and the corresponding transmittance was ranging from 51.29% to 68.97%. For the applications, the luminance values of LED with the AgNWs film as electrodes was higher than that with commercial silver colloid electrodes. The AgNWs show great potential to be applied as electrode materials. In the near future, it is possible to use this method to fabricate other composite nanomaterials for applications on nanometer-scale electronics, optoelectronics, and sensing devices.

Acknowledgements

The author is grateful to the National Science Council of Taiwan for the funding of this research through Grant No. NSC 103-2221-E-110 -009 -MY3.

References

[1] J.Y. Zou, H.L. Yip, S.K. Hau, A.K.Y. Jen, Metal grid/conducting polymer hybrid transparent electrode for inverted polymer solar cells, Appl. Phys. Lett. 96 (2010).
[2] S. Bae, H. Kim, Y. Lee, X. Xu, J.S. Park, Y. Zheng, et al., Roll-to-roll production of 30-inch graphene films for transparent electrodes, Nat. Nanotechnol. 5 (Aug 2010) 574–578.
[3] B. Meng, W. Tang, Z.H. Too, X.S. Zhang, M.D. Han, W. Liu, et al., A transparent single-friction-surface triboelectric generator and self-powered touch sensor, Energy Environ. Sci. 6 (Nov 2013) 3235–3240.

[4] S. Takamatsu, T. Takahata, M. Muraki, E. Iwase, K. Matsumoto, I. Shimoyama, Transparent conductive-polymer strain sensors for touch input sheets of flexible displays, J. Micromech. Microeng. 20 (2010).
[5] S. Takamatsu, T. Takahata, K. Matsumoto, I. Shimoyama, Micro-patterning of a conductive polymer and an insulation polymer using the Parylene lift-off method for electrochromic displays, J. Micromech. Microeng. 21 (2011) 075021.
[6] N. Yamamoto, H. Makino, S. Osone, A. Ujihara, T. Ito, H. Hokari, et al., Development of Ga-doped ZnO transparent electrodes for liquid crystal display panels, Thin Solid Films 520 (2012) 4131–4138.
[7] C.J.M. Emmott, A. Urbina, J. Nelson, Environmental and economic assessment of ITO-free electrodes for organic solar cells, Sol. Energy Mater. Solar Cells 97 (2012) 14–21.
[8] Y. Lin, H.F. Dam, T.R. Andersen, E. Bundgaard, W. Fu, H. Chen, et al., Ambient roll-to-roll fabrication of flexible solar cells based on small molecules, J. Mater. Chem. C 1 (2013) 8007.
[9] L. Hu, J. Li, J. Liu, G. Gruner, T. Marks, Flexible organic light-emitting diodes with transparent carbon nanotube electrodes: problems and solutions, Nanotechnology 21 (2010) 55202.
[10] T.M. Barnes, J.D. Bergeson, R.C. Tenent, B.A. Larsen, G. Teeter, K.M. Jones, et al., Carbon nanotube network electrodes enabling efficient organic solar cells without a hole transport layer, Appl. Phys. Lett. 96 (2010) 243309.
[11] H. Park, P.R. Brown, V. Bulovic, J. Kong, Graphene as transparent conducting electrodes in organic photovoltaics: studies in graphene morphology, hole transporting layers, and counter electrodes, Nano Lett. 12 (2012) 133–140.
[12] Z. Yu, Q. Zhang, L. Li, Q. Chen, X. Niu, J. Liu, et al., Highly flexible silver nanowire electrodes for shape-memory polymer light-emitting diodes, Adv. Mater. 23 (2011) 664–668.
[13] J.Y. Lee, S.T. Connor, Y. Cui, P. Peumans, Solution-processed metal nanowire mesh transparent electrodes, Nano Lett. 8 (Feb 2008) 689–692.
[14] T. Kim, A. Canlier, G.H. Kim, J. Choi, M. Park, S.M. Han, Electrostatic spray deposition of highly transparent silver nanowire electrode on flexible substrate, ACS Appl. Mater. Interf. 5 (Feb 2013) 788–794.
[15] S. Coskun, B. Aksoy, H.E. Unalan, Polyol synthesis of silver nanowires: an extensive parametric study, Cryst. Growth Des. 11 (2011) 4963–4969.
[16] Y.M. Shin, M.M. Hohman, M.P. Brenner, G.C. Rutledge, Electrospinning: a whipping fluid jet generates submicron polymer fibers, Appl. Phys. Lett. 78 (2001) 1149.
[17] D. Li, Y. Wang, Y. Xia, Electrospinning nanofibers as uniaxially aligned arrays and layer-by-layer stacked films, Adv. Mater. 16 (2004) 361–366.
[18] A. Frenot, I.S. Chronakis, Polymer nanofibers assembled by electrospinning, Curr. Opin. Colloid Interf. Sci. 8 (Mar 2003) 64–75.
[19] Z. Gaofeng, L. Wenwang, W. Xiang, W. Han, S. Daoheng, L. Liwei, Experiment and simulation of coiled nanofiber deposition behavior from near-field electrospinning, in: Nano/Micro Engineered and Molecular Systems (NEMS), 2010 5th IEEE International Conference on, 2010, pp. 284–288.
[20] D. Sun, C. Chang, S. Li, L. Lin, Near-field electrospinning, Nano Lett. 6 (Apr 2006) 839–842.
[21] C. Chang, K. Limkrailassiri, L. Lin, Continuous near-field electrospinning for large area deposition of orderly nanofiber patterns, Appl. Phys. Lett. 93 (2008) 123111.
[22] Z.Y. Ou, Z.H. Liu, C.T. Pan, L.W. Lin, Y.J. Chen, H.W. Lai, Study on piezoelectric properties of near-field electrospinning PVDF/MWCNT nano-fiber, in: Nano/Micro Engineered and Molecular Systems (NEMS), 2012 7th IEEE International Conference on, 2012, pp. 125–128.
[23] Z.H. Liu, C.T. Pan, L.W. Lin, J.C. Huang, Z.Y. Ou, Directwrite PVDF nonwoven fiber fabric energy harvesters via the hollow cylindrical nearfield electrospinning process, Smart Mater. Struct. 23 (2014).
[24] Z.H. Liu, C.T. Pan, L.W. Lin, H.W. Lai, Piezoelectric properties of PVDF/MWCNT nanofiber using near-field electrospinning, Sens. Actuat. A: Phys. 193 (2013) 13–24.
[25] D. Di Camillo, F.R., S. Santucci, L. Lozz, Department of Physics (Italy), C. Cantalini, L. Giancaterini, Department of Chemistry and Materials (Italy). Preparation of Nitrogen doped TiO_2 nanofibers by Near Field Electrospinning (NFES) technique for NO_2 sensing, in: The 14th International Meeting on Chemical Sensors, 2012.
[26] S.Y. Min et al., Large-scale organic nanowire lithography and electronics, Nat. Commun. 4 (2013) 1773.
[27] D. Di Camillo et al., Near-field electrospinning of light-emitting conjugated polymer nanofibers, Nanoscale 5 (23) (2013) 11637–11642.
[28] C. Mayousse et al., Improvements in purification of silver nanowires by decantation and fabrication of flexible transparent electrodes. Application to capacitive touch sensors, Nanotechnology 24 (21) (2013) 215501.
[29] N.V. Nghia, N.N.K. Truong, N.M. Thong, N.P. Hung, Synthesis of nanowire-shaped silver by polyol process of sodium chloride, Int. J. Mater. Chem. 2 (2012) 75–78.
[30] H.S. Wang, X.L. Qiao, J.G. Chen, X.J. Wang, S.Y. Ding, Mechanisms of PVP in the preparation of silver nanoparticles, Mater. Chem. Phys. 94 (2005) 449–453.
[31] J. Song, M. Chen, M.B. Olesen, C. Wang, R. Havelund, Q. Li, et al., Direct electrospinning of Ag/polyvinylpyrrolidone nanocables, Nanoscale 3 (Dec 2011) 4966–4971.
[32] T. Araki et al., Low haze transparent electrodes and highly conducting air dried films with ultra-long silver nanowires synthesized by one-step polyol method, Nano Res. 7 (2) (2014) 236–245.